Transfer hydrogenolysis of aromatic ethers promoted by the bimetallic Pd/Co catalyst

F. Mauriello[1,*], H. Ariga-Miwa[2], E. Paone[1], R. Pietropaolo[1], S. Takakusagi[2], and K. Asakura[2,*]

[1] *Dipartimento DICEAM, Università Mediterranea di Reggio Calabria, Loc. Feo di Vito, I-89122 Reggio Calabria, Italy*

[2] *Institute of Catalysis, Hokkaido University, Kita-ku N21W10, Sapporo, Hokkaido 001-0021, Japan*

**Corresponding authors.*

Tel: +39-0965-1692278; Fax: +39-0965-1692201
E-mail: francesco.mauriello@unirc.it. (F. Mauriello)

Tel: +81-11-7069113; Fax: +81-11-7069113
E-mail: askr@cat.hokudai.ac.jp (K. Asakura)

Keywords: transfer hydrogenolysis; lignin; aromatic ethers; heterogeneous catalysis; palladium; cobalt;

Abstract

The transfer hydrogenolysis of lignin derived aromatic ethers (benzyl phenyl ether, phenethyl phenyl ether and diphenyl ethers) have been investigated by using the coprecipitated Pd/Co as heterogeneous catalyst and 2-propanol as H-donor/solvent. A quantitative conversion of benzyl phenyl ether into toluene and cyclohexanol was obtained after 180 minutes at 240 °C. The bimetallic Pd/Co catalyst is, by far, more efficient if compared to commercial Pd/C and Co-based catalytic systems showing, at the same time, a good reusability. The enhanced ability in the C-O bond cleavage in aromatic ethers is related to the formation of bimetallic Pd-Co ensembles, arisen from the preparation procedure adopted, as confirmed by a complete physico-chemical characterization that includes XRD, SEM, TEM, H_2-TPR, XPS and EXAFS analysis.

1. Introduction

The use of lignocellulosic biomasses for the sustainable production of renewable energy, fuels and chemicals is unquestionably known [1-3]. The key constituents of lignocellulose (cellulose, hemicellulose and lignin) are characterized by a chemical structure that can provide starting substrates for the preparation of a vast variety of building block chemicals. Cellulose and hemicellulose can be first depolymerized into C6-C5 sugars and then converted into short-chain alcohols, polyols, esters and acids [4]. On the other hand, lignin is the only lignocellulosic component that allows the production of bio-based aromatic compounds [5]. Renewable aromatics will constitute a significative quota of the future global bioeconomy due to their wide-ranging industrial applications including polymers, textiles, paints, tires, coatings, fragrances and pharmaceuticals [6].

One of the most adopted chemical approaches to lignin depolymerization is surely the hydrogenolysis technique (the direct C-O bond cleavage by means of molecular H_2) that, allowing also the efficient reduction of the oxygen content in lignocellulosic constituents and their chemical derivatives, is becoming one of the core technologies in the modern bio-refinery [7]. Therefore, the basic chemistry of C-O bond breaking of aromatic ethers is still one of the fundamental tasks to accomplish in order to selective produce chemicals from lignin [8].

However, in hydrogenolysis reactions, the "lysis" of carbon–carbon or carbon–heteroatom bonds is generally promoted by homogeneous or heterogeneous catalysts in presence of high-pressure molecular hydrogen (H_2 is poorly soluble in most reaction solvents) with all associated problems including security hazards, expensive infrastructures, purchase and transport of the explosive gas.

In the last years, a significant growth to an alternative catalytic approach avoiding the direct use of molecular hydrogen was observed [9, 10]. To this regard, the catalytic transfer hydrogenolysis (CTH) may represent a valid green alternative to classic hydrogenation/hydrogenolysis reactions owing to the use of indirect H-source molecules [11]. Simple organic molecules including short chain alcohols (2-propanol, ethanol and methanol) and acids (formic acid) can be efficiently used as H-donor for CTH

reactions. At the same time, CTH molecules are generally easily to handle, potentially obtainable from renewable feedstocks and, due to their lower tendency to release hydrogen, may allow a higher production of aromatic compounds from lignin and its derived molecules.

In the last years, several authors used different homogeneous and heterogeneous catalysts for the hydrogenolysis and transfer hydrogenolysis of lignin and lignin-derived ethers [12-18]. In particular, the commercial Pd/C has attracted a lot of research interests allowing an efficient transformation of lignin and of a variety of aromatic ethers using formic acid and 2-propanol as H-donors [19-21].

Nevertheless, it is well known that the introduction of a second metal is helpful to increase the catalytic performances [22-24]. For instance, the addition of iron to palladium, through the co-precipitation technique, produces intimate metal-support interactions that create a synergistic effect enabling a higher reactivity in several important reactions including the CTH of aromatic ethers [25-30]. In recent years, we investigated the CTH of glycerol also by using the co-precipated Pd/Co catalyst under mild operating conditions [31-33]. This was found to be definitely the most efficient coprecipitated Pd based catalyst in the C-O bond cleavage in biomass derived polyols.

In this paper, we evaluate the performance of the co-precipitated Pd/Co catalyst in the CTH of benzyl phenyl ether (BPE), 2-phenethyl phenyl ether (PPE) and diphenyl ether (DPE) that represent the simplest lignin-derived aromatic ethers and can be used to mimic the catalytic cleavage of the most common lignin linkages (Scheme 1). A throughout physisco-chemical characterization by means of XRD, SEM-EDX, TEM, H_2-TPR, XPS and EXAFS analysis highlights the presence of bimetallic Pd-Co ensembles that positively promote the C-O bond cleavage of the investigated aromatic ethers. If compared with the commercial Pd/C and other benchmark cobalt-based systems (metallic Co, CoO and Co_3O_4), the bimetallic Pd/Co catalyst shows higher activity. Moreover, it can be recycled up to six times without any activity loss and easily recovered from the reaction medium magnetically.

Scheme 1 about here

2. Experimental Section

2.1 Catalysts preparation

2-Phenethyl phenyl ether (PPE) was purchased from Frinton Laboratories (USA). All other chemicals were purchased from Carlo Erba Reagents (Italy) and used without additional purification.

The Pd/Co catalyst (with nominal palladium loading of 5 wt%) was prepared on using the co-precipitation technique. The dropwise addition of an aqueous solution of palladium (II) nitrate and cobalt (II) nitrate hexahydrate into an aqueous solution of Na_2CO_3 (1M) allows the formation of a solid purple product that was filtered, washed with deionized water until neutral pH was reached and dried overnight at 120°C. The dried powder was then oxidized at 300°C for 3 hours under an air flow and, before use, reduced at 300°C for 2 h under a hydrogen flow.

2.2 Catalysts Characterization.

XRD data were acquired at room temperature on a Bruker D2 PHASER diffractometer (Ni β-filtered Cu Kα radiation; λ=0.15418 nm; 2θ range=20–80°; scan speed=0.5°min^{-1}).

XRF analysis were performed with a Bruker Tracer IV-SD Spectrometer (40 keV, 15 μA over 15 s with peak assignment based on alignment with K-line energy transitions).

SEM-EDX analysis were carried out on a Phenom Pro-X scanning electron microscope (SEM) equipped with an energy-dispersive X-ray (EDX). EDX analysis was used to estimate the content and the dispersion of metals, acquiring, for all samples, at least 20 points for 3 different magnifications.

The particle size and the relative morphology of investigated catalysts were analysed by performing Transmission Electron Miscroscopy (TEM) measurements using a JEM-2100F (JEOL, Japan) operating at an acceleration voltage of 200 kV and directly interfaced with a computer controlled-CCD for real-time image processing. Several hundred particles were counted on the micrographs and the average diameter was calculated by using the expression: $d_n = \Sigma n_i d_i / n_i$ where n_i is the number of particles of diameter d_i.

H_2-TPR measurements were performed using a conventional TPR apparatus by heating 50mg of oxidated samples at a linear rate of 10 °C min^{-1} from 0 to 1000 °C in a 5vol % of H_2/Ar mixture at a flow rate of 20 cm^3 min^{-1}. The H_2 consumption was determined with a thermal conductivity detector (TCD).

XPS measurements were performed on a JPS-9010MC photoelectron spectrometer containing an Al Kα (1486.6 eV) radiation source. After the reduction treatment, samples were introduced into the XPS chamber, avoiding exposure to air. All spectra were recorded at room temperature, and the binding energies (BE) were determined taking the C 1s peak at 284.6 eV as reference.

Extended X-ray absorption fine structure (EXAFS) spectra of the Pd/Co catalyst were measured at the Photon Factory of the Institute for Materials Structure Science, High Energy Accelerator Research Organization - KEK (Tsukuba, Japan). Co-K and Fe-K edge XANES/EXAFS spectra for the catalysts were obtained using a Si(111) monochromator with beam line BL9A of PF (2.5 GeV,450 mA) and Pd K-edge spectra were obtained using a Si(311) monochromator with beam line MW10A of PF-AR (6.5 GeV,100mA). Analysis of the EXAFS data was performed using the REX2000 (Rigaku Co.) analysis program.

2.3 Catalytic Tests.

Reactions were carried out in a 100 ml stainless steel autoclave at a stirring speed of 500 rpm. The reactor, containing the reduced catalyst (0.125 g) suspended in a 0.1 M solution of the chosen substrate in 2-propanol (40 mL), was purged three times with N_2 (99.99%), successively pressurized at the desired gas (N_2 or H_2) pressure and finally heated at the necessary reaction temperature. At the end of every reaction, the system was cooled down and, when at room temperature, the pressure was prudently released, and the liquid phase was analyzed using an off-line gas chromatograph (Agilent 6890N equipped with CP-WAX 52CB, 60 m, i.d. 0.53 mm).

In all recycling tests, after any run, the catalyst was first recovered, carefully washed with 2-propanol, and reused under the same reaction conditions.

The conversion, product selectivity and product yield in the liquid phase were calculated on the basis of the following equations:

$$\text{Conversion [\%]} = \frac{\text{mol of reacted substrate}}{\text{mol of substrate feed}} \times 100 \quad (1)$$

$$\text{Liquid phase selectivity [\%]} = \frac{\text{mol of specific product in liquid phase}}{\text{sum of mol of all products in liquid phase}} \times 100 \quad (2)$$

$$\text{Product Yield [\%]} = \frac{\text{mol of specific product}}{\text{mol of substrate feed}} \times 100 \quad (3)$$

3. Results and Discussion

3.1 Catalyst preparation and characterization

The Pd/Co catalyst was prepared through the co-precipitation of palladium nitrate and cobalt nitrate hexahydrate, simultaneously added dropwise into a 1 M aqueous solution of Na_2CO_3. The precipitated solid, after filtration, was washed several times with distilled water until a neutral pH was reached, dried overnight at 120°C, calcinated at 300°C in air and finally reduced under a flow of molecular hydrogen at 300°C. Table 1 reports the main characteristic of the Pd/Co catalyst.

Table 1 about here

Figure 1 about here

The X-ray powder diffraction (XRD) pattern of the unreduced Pd/Co catalyst shows diffraction peaks typical of pure cubic crystalline Co_3O_4 (Figure 1, up) [34]. The spectrum of the sample, after reduction, shows diffraction peaks of the hexagonal metallic cobalt indicating the promoting effect of Pd in the support reduction (Figure 1, down). This point is worth of remark since the complete reduction of Co_3O_4 into metallic Co in H_2 atmosphere generally occurs up to 400°C [35].

Highly dispersed palladium particles are easily detected by SEM-EDX analysis (Figure 2) [36].

Figure 2 about here

Representative TEM images of reduced Pd/Co catalyst are reported in Figure 3 where distinctive lattice fringes with an interplanar distance of 0.19 nm, typical of the (111) plane of the metallic cobalt [37], can be easily detected confirming the complete reduction of the support. Smaller darker nanoparticles were identified, also on the basis of the following EXAFS analysis (see below), as bimetallic Pd-Co systems [38-39] with a particles size distribution of about 8.7 nm.

Figure 3 about here

Figure 4 includes the H_2-TPR profile of the Pd/Co sample, characterized by only one broad and intense peak centered at about 260°C that can be related to the simultaneous reduction of both palladium and cobalt cations. Most important, the main H_2-TPR reduction peak of the Pd/Co sample (Figure 4) is shifted to lower temperatures of about 150°C than that of the Co_3O_4 sample (prepared by the identical synthetic procedure: precipitation) that is characterized by a wide non symmetric peak that includes both $Co_3O_4 \rightarrow CoO$ and $CoO \rightarrow Co$ reductions [40, 41]. This phenomenon is well known and is commonly ascribed to the promoting effect of well-dispersed palladium particles on the Co_3O_4 reduction indicating a strong interaction between Pd ions and the metal oxide support [42].

Figure 4 about here

The XPS spectrum of the reduced Pd/Co catalyst shows that the binding energy of the Pd $3d_{5/2}$ level appears at about 0.5 eV value higher than that of the binding energy of metallic palladium, indicating

the presence of partial positively charged Pd species suggesting the formation of a Pd-Co alloy (Figure 5) [43, 44]. At the same time, the presence of metallic cobalt is confirmed by its typical sharp peak at 778.2 eV [45].

Figure 5 about here

The main results of extended X-ray absorption fine structure (EXAFS) characterization at the Pd K-edge are reported in Table 2. In the Pd/Co catalyst, the most marked feature is the observation of a shorter scattering Pd-Co path of 2.51 Å compared with the Pd–Pd distance of about 2.70 Å that confirms the formation of Pd-Co bimetallic ensembles [46-47].

Table 2 about here

3.2 Catalytic tests

Table 3 includes catalytic results of Pd/Co and Pd/C catalysts, in the transfer hydrogenolysis of BPE.

Table 3 about here

After 3 hours of reaction, a high BPE conversion at 210°C (88%) and a total conversion (100%) at 240°C evidence the excellent performance of the Pd/Co catalyst. The products distribution pattern changes within the investigated temperature range. Indeed, at the lower temperature (180°C), the only products observed are toluene (TOL) and phenol (PHE). When the temperature increases, phenol is progressively converted into cyclohexanol (CXO) that becomes, at 240°C, the main reaction product together with toluene. This has not to be considered a disfavouring result since it is worth to highlight

that cyclohexanol is an important feedstock in the industrial chemistry being used as a precursor to nylons, plastics, detergents and insecticides.

On the contrary, the commercial Pd/C exhibits a significant lower activity. Indeed, at 210°C the BPE conversion is less than 20% and the maximum is 45% at 240°C, the highest temperature investigated (Table 1). The modest performance of the commercial Pd/C catalyst, in CTH reactions, was already reported and attributed to its lower ability to dehydrogenate 2-propanol [26, 31].

Pure metallic cobalt, CoO and Co_3O_4 were also tested within the same temperature range and no BPE conversion was found, clearly indicating that palladium presence in the catalyst is essential for the C–O bond breaking. The lack of any noteworthy reactivity using either Pd/C or Co-based catalysts, confirms that the marked activity shown by the bimetallic Pd/Co catalyst has to be attributed to the strong interaction between palladium and cobalt, as consequence of the preparation method (co-precipitation) in analogy with other reports [31, 33, 46].

At the same time, it is worth to underline that reactions carried out in absence of any catalyst do not give any BPE conversion, implying that (i) the non-catalyzed pyrolysis of aromatic ethers does not occur under the adopted conditions [48] and that (ii) the presence of an appropriate catalyst is crucial for C–O bond breaking.

CTH of BPE investigation, at different reaction times (Figure 6), at 210°C (the best reaction temperature that maximizes aromatic production) was also carried out. The BPE conversion was completed after 6 h of reaction, and toluene yields progressively increase on increasing reaction times, reaching a maximum value at 360 min. However, no hydrogenation into methylcyclohexane was, in any case, registered. On the other hand, the highest yield of phenol was reached after 180 min and then it progressively decreases because of further hydrogenation into cyclohexanol.

Figure 6 about here

The reusability of the Pd/Co catalyst was also evaluated under the harsh reaction condition adopted (240°C for 3 hours). Pd/Co maintains its high activity after six consecutive recycling runs and no changes in product selectivity was found (Figure 7). This result clearly highlights the good stability of the catalyst that, additionally, can be easily recovered from the reaction medium magnetically.

Figure 7 about here

The substrate scope was subsequently extended to additional aromatic ethers representative of lignin linkages, namely, PPE and DPE both under CTH conditions as well as under classical hydrogenolysis conditions (Figure 8). Catalytic tests show that: (i) improved conversions can be easily achieved in presence of molecular hydrogen and (ii) the cleavage of the C-O bond of PPE and DPE is less efficient due to the higher bond dissociation energies (β-O-4 = 289 kJ/mol and 4-O-5 = 314 kJ/mol) involved [49-50].

Figure 8 about here

4. Conclusions

The catalytic conversion of lignin-deriving aromatic ethers (benzyl phenyl ether, 2-phenethyl phenyl ether and diphenyl ether) was investigated under transfer hydrogenolysis conditions over the bimetallic Pd/Co catalyst by using 2-propanol as solvent/H-donor.

The bimetallic Pd/Co catalyst, prepared by the coprecipitation technique, is able to effectively cleave the C−O bond of benzyl phenyl ether (α-O-4 lignin model molecule) that, after 3 hours at 240°C, is selectively converted into toluene and cyclohexanol. Six consecutive recycling tests in the transfer hydrogenolysis of BPE proved the good stability of the Pd/Co catalyst that can be easily recoverable

magnetically. The CTH of 2-phenethyl phenyl ether and diphenyl ether were found to be less efficient due to the higher bond dissociation energies involved in the C-O bond breaking.

Physicochemical characterizations clearly demonstrate the presence of bimetallic Pd/Co ensembles (alloy-type) as a crucial factor involved in the observed enhancement of the catalytic activity.

Acknowledgment

The authors gratefully acknowledge financial support from the Università Mediterranea di Reggio Calabria (Italy) and the Photon Factory Program Advisory Committee of the Photon Factory of the Institute for Materials Structure Science, High Energy Accelerator Research Organization - KEK (Tsukuba, Japan) for providing beam time for XANES/EXAFS analysis ("Structural characterization of coprecipitated palladium-iron oxide catalysts for the selective hydrogenolysis of C-O bond in biomass derived compounds", Approved Proposal n°2014000053).

References

[1] M. Besson, P. Gallezot, C. Pinel, Chem. Rev. 114 (2014) 1827−1870.

[2] C.O. Tuck, E. Peréz, I.T. Horvaťh, R.A. Sheldon, M. Poliakoff, Science 337 (2012) 695−699.

[3] C.-H. Zhou, X. Xia, C.-X. Lin, D.-S. Tong, J. Beltramini, Chem. Soc. Rev. 40 (2011) 5588−5617.

[4] I. Delidovich, K. Leonhard, R. Palkovits, Energy Environ. Sci. 7 (2014) 2803-2830.

[5] C. Xu, R. A. D. Arancon, J. Labidi, R. Luque, Chem. Soc. Rev. 43 (2014) 7485−7500.

[6] OECD (2014), "Biobased Chemicals and Bioplastics: Finding the Right Policy Balance", OECD Science, Technology and Industry Policy Papers, No. 17, OECD Publishing. http://dx.doi.org/10.1787/5jxwwfjx0djf-en

[7] A. M. Ruppert, K. Weinberg, R. Palkovits, Angew. Chem., Int. Ed. 51 (11) (2012) 2564−2601.

[8] M. Zaheer, R. Kempe, ACS Catal. 5 (2015) 1675−1684.

[9] D. Wang, D. Astruc, Chem. Rev. 115 (13) (2015) 6621−6686.

[10] M. J. Gilkey, E. X. Bingjun, ACS Catal. 6 (2016) 1420−1436.

[11] C. Espro, B. Gumina, T. Szumelda, E. Paone, F. Mauriello, Catalysts, 8 (8) (2018) 313.

[12] A. G. Sergeev, J. F. Hartwig, Sciencec332 (2011) 439−443.

[13] X. Wang, R. Rinaldi, Energy Environ. Sci. 5 (8) (2012) 8244−8260.

[14] X. Wang, R. Rinaldi, Angew. Chem., Int. Ed. 52 (2013) 11499−11503.

[15] G. S. Macala, T. D. Matson, C. L. Johnson, R. S. Lewis, A. V. Iretskii, P. C. Ford, ChemSusChem 2 (2009) 215−217.

[16] K. Barta, T. D. Matson, M. L. Fettig, S. L. Scott, A. V. Iretskii, P. C. Ford, Green Chem. 12 (2010) 1640−1647.

[17] F. Mauriello, E. Paone, R. Pietropaolo, A.M. Balu, R. Luque, ACS Sustain Chem Eng 6 (7) (2018) 9269–9276.

[18] M. Guo, J. Peng, Q. Yang, C. Li, ACS Catal. 8 (2018) 11174–11183.

[19] M. V. Galkin, S. Sawadjoon, V. Rohde, M. Dawange, J. S. M. Samec, ChemCatChem 6 (1) (2014) 179−184.

[20] M. V. Galkin, J. S. M. Samec, ChemSusChem 7 (8) (2014) 2154− 2158.

[21] M. V. Galkin, C. Dahlstrand, J. S. M. Samec, ChemSusChem 8 (2015) 2187−2192.

[22] D.M. Alonso, S.G. Wettstein, J.A. Dumesic, Chem. Soc. Rev. 41 (2012) 8075–8098.

[23] J.-w. Zhang, Y. Cai, G.-p. Lu, C. Cai, Green Chem. 18 (2016) 6229−6235.

[24] J. Zhang, J. Teo, X. Chen, H. Asakura, T. Tanaka, K. Teramura, N. Yan, ACS Catal. 4 (2014) 1574−1583.

[25] C. Espro, B. Gumina, E. Paone, F. Mauriello, Catalysts 7 (2017) 78.

[26] E. Paone, C. Espro, R. Pietropaolo, F. Mauriello, Catal. Sci. Technol. 6 (22) (2016) 7937−7941.

[27] B. Gumina, F. Mauriello, R. Pietropaolo, S. Galvagno, C. Espro, Molecular Catalysis, 446 (2018) 152–160.

[28] D. Cozzula, A. Vinci, F. Mauriello, R. Pietropaolo, T.E. Müller, ChemCatChem 8 (2016) 1515–1522.

[29] M.G. Musolino, L.A. Scarpino, F. Mauriello, R. Pietropaolo, Green Chem. 11 (2009) 1511–1513.

[30] B. Gumina, C. Espro, S. Galvagno, R. Pietropaolo, F. Mauriello, ACS Omega 4 (2019) 352-357.

[31] F. Mauriello, H. Ariga, M. G. Musolino, R. Pietropaolo, S. Takakusagi, K. Asakura, Appl. Catal., B 166 (2015) 121−133.
[32] M. G. Musolino, C. Busacca, F. Mauriello, R. Pietropaolo, Appl. Catal., A 379 (2010) 77−86.
[33] M. G. Musolino, L. A. Scarpino, F. Mauriello, R. Pietropaolo, ChemSusChem 4 (8) (2011) 1143−1150.
[34] International Center for Diffraction Data, Powder Diffraction Database, Penn- sylvania, PA, 1997.
[35] B. A. Sexton, A. E. Hughes, T. W. Turney, J. Catal. 97 (1986) 390-406.
[36] L.S.F. Feio, C.E. Hori, L.V. Mattos, D. Zanchet, F.B. Noronha, J.M.C. Bueno, App. Catal. A: Gen. 348 (2008) 183–192.
[37] D. Li, L. Zhang, H. Chen, L-X. Ding, S. Wanga, H. Wang, Chem.Commun. 51 (2015) 16045-16048;
[38] S. Nandi, P. Patel, N. H. Khan, A. V. Biradar, R. I. Kureshy, Inorg. Chem. Front. 5 (2018) 806-813
[39] Y. Yao, L. L. Gu, W. Jiang, H. C. Sun, Q. Su, J. Zhao, W. J. Ji and C. T. Au, Catal. Sci. Technol. 6 (2016) 2349-2360
[40] Q. Liu, L.-C. Wang, M. Chen, Y. Cao, H.-Y. He, K.-N. Fan, J. Catal. 263 (2009) 104-113
[41] F.B. Noronha, M. Schmal, C. Nicot, B. Moraweck, R. Fréty, J. Catal. 168 (1997) 42–50.
[42] M.L. Cubeiro, J.L.G. Fierro, J. Catal. 179 (1998) 150–162.
[43] Y-S. Fenga, X-Y. Lina, J. Haoa, H-J. Xu, Tetrahedron 70 (2014) 5249-5253.
[44] C.D. Wanger, W.M. Riggs, L.E. Davis, J.F. Moulder, G.E. Muilenberg, Handbook of X-ray Photoelectron Spectroscopy, Perkin-Elmer Corp., Minnesota, USA, 1979.
[45] B. Mierzwa, Z. Kaszkur, B. Moraweck, J. Pielaszek, J. Alloys Compd 286 (1999) 93–97.
[46] F. Liao, T. W. B. Lo, J. Qu, A. Kroner, A. Dent, S. C. E. Tsang, Catal. Sci. Technol. 5 (2015) 3491-3495
[47] L. Nguyen, S. Zhang, L. Wang, Y. Li, H. Yoshida, A. Patlolla, A.I. Frenkel, S. Takeda, F.F. Tao, ACS Catal. 6 (2) (2016) 840–850.
[48] J. He, L. Lu, C. Zhao, D. Mei, J. A. Lercher, J. Catal. 311 (2014) 41–51.
[49] E. Dorrestijn, L. J. J. Laarhoven, I. W. C. E. Arends, P. Mulder, J. Anal. Appl. Pyrolysis 54 (1−2) (2000) 153−192.
[50] R. Parthasarathi, R. A. Romero, A. Redondo, S. Gnanakaran, J. Phys. Chem. Lett. 2 (20) (2011) 2660−2666.

Figure captions

Scheme 1. Benzyl Phenyl Ether (BPE), 2-Phenethyl Phenyl Ether (PPE) and Diphenyl Ether (DPE): the simplest lignin-derived aromatic ethers.

Figure 1. XRD profiles of unreduced (down) and reduced (up) Pd/Co catalyst.

Figure 2. SEM-EDX characterization of Pd/Co catalyst.

Figure 3. TEM image of the Pd/Co catalyst.

Figure 4. H_2-TPR profiles of unreduced Pd/Co and Co_3O_4 catalysts.

Figure 5. XPS plots of the reduced Pd/Co catalyst in Co $2p_{3/2}$ and Pd $3d_{5/2}$ levels.

Figure 6. Product yields in the conversion of BPE with the Pd/Co catalyst under transfer hydrogenolysis conditions at 210°C against time (reaction conditions: 0.125 g of catalyst; 40 ml solution of BPE 0.1 M; N_2 pressure: 10 bar; stirring: 500 rpm).

Figure 7. Recycling tests for Pd/Co catalyst in the CTH of BPE (reaction conditions: 0.125 g of catalyst; 40 ml solution of BPE 0.1 M; temperature: 240°C; time: 180 minutes; N_2 pressure: 10 bar; stirring: 500 rpm).

Figure 8. Conversion in the CTH and in the hydrogenolysis of BPE, PPE, and DPE (reaction conditions: 0.125 g of catalyst; 40 ml solution of BPE 0.1 M; temperature: 240°C; time: 180 minutes; N_2 or H_2 pressure: 10 bar; stirring: 500 rpm)

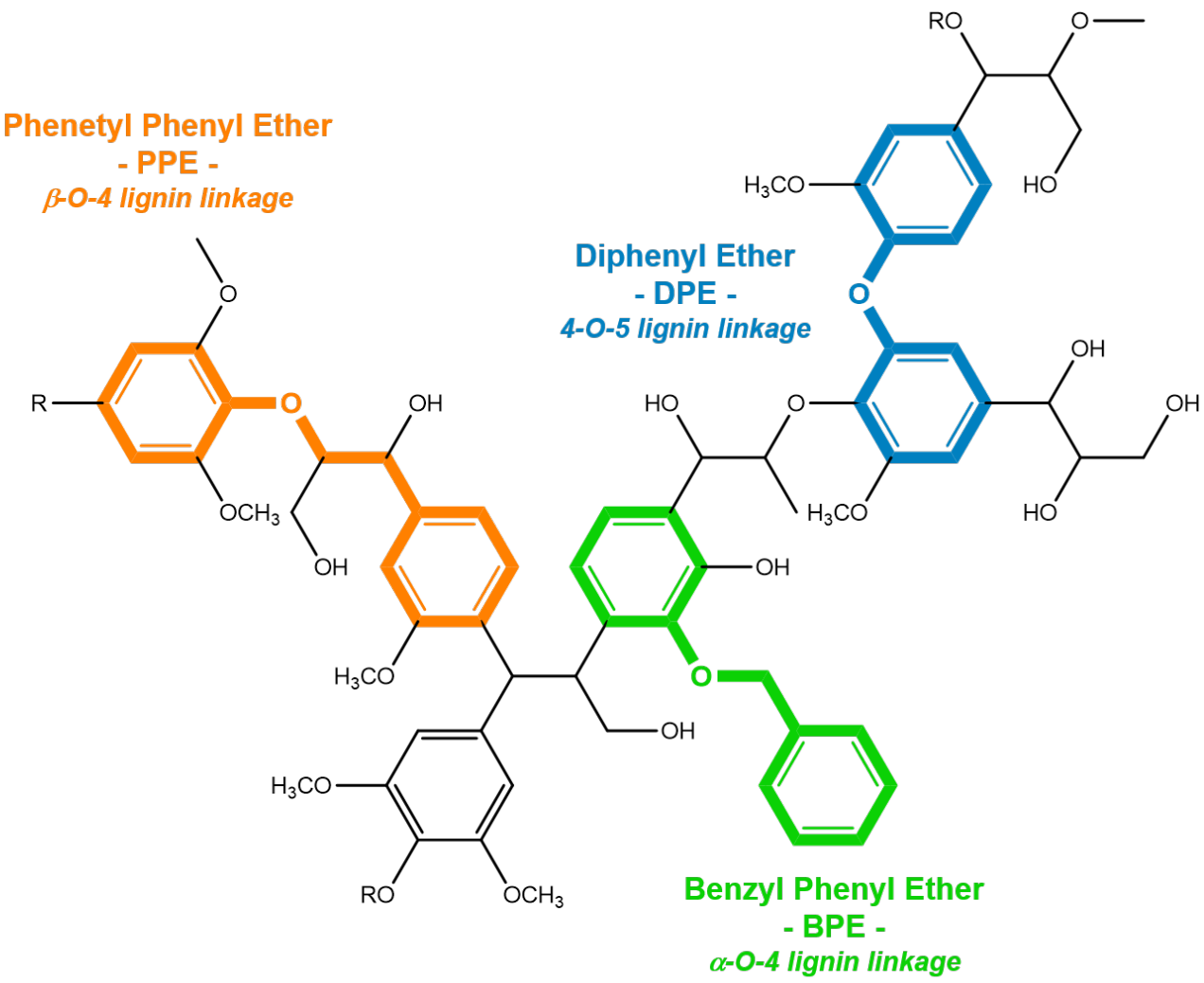

Scheme 1 Benzyl Phenyl Ether (BPE), 2-Phenethyl Phenyl Ether (PPE) and Diphenyl Ether (DPE): the simplest lignin-derived aromatic ethers.

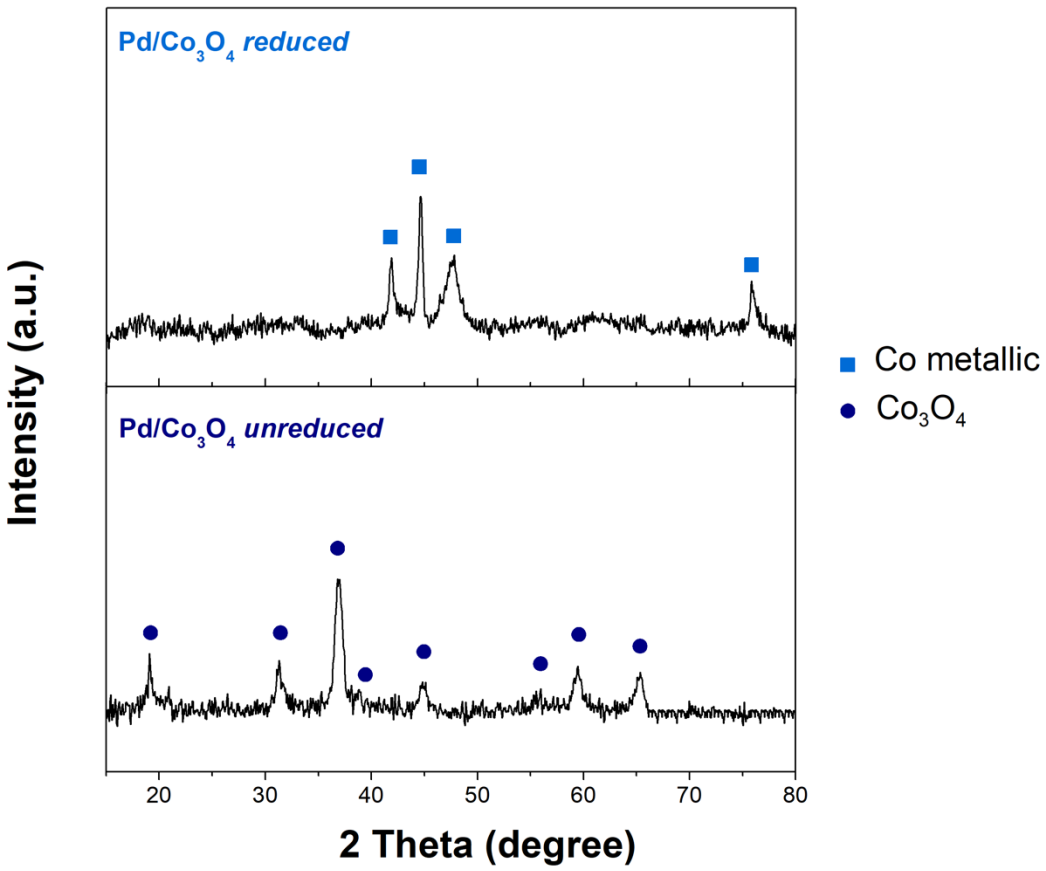

Figure 1 XRD profiles of unreduced (down) and reduced (up) Pd/Co catalyst.

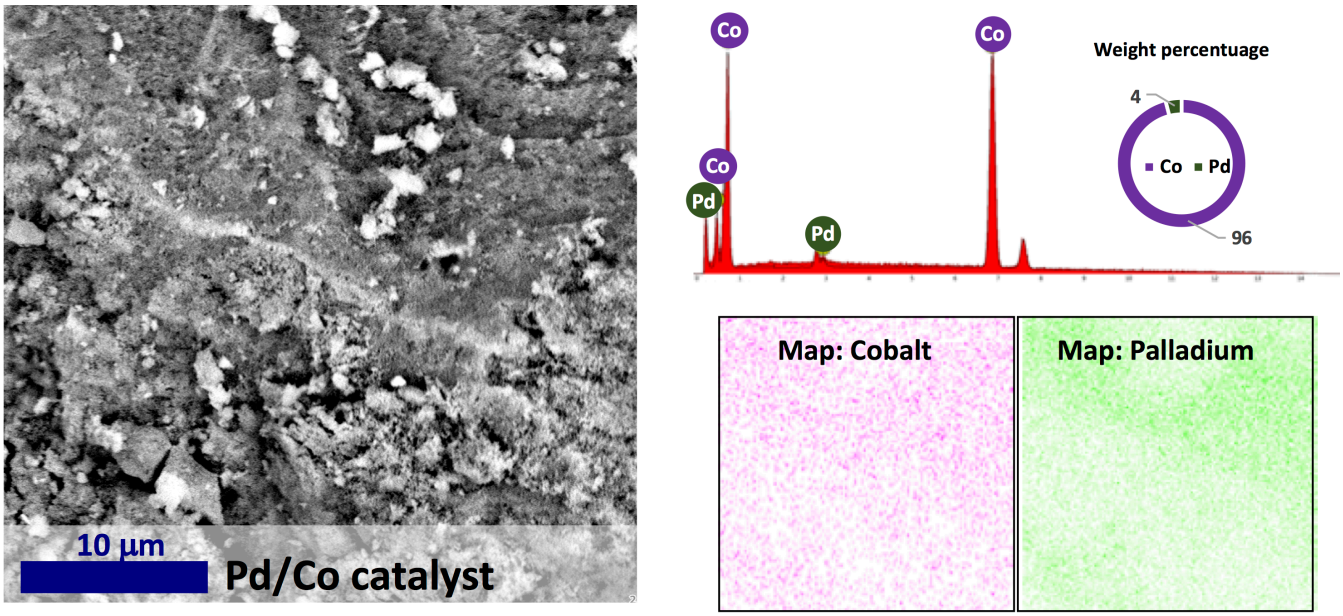

Figure 2 SEM-EDX characterization of Pd/Co catalyst.

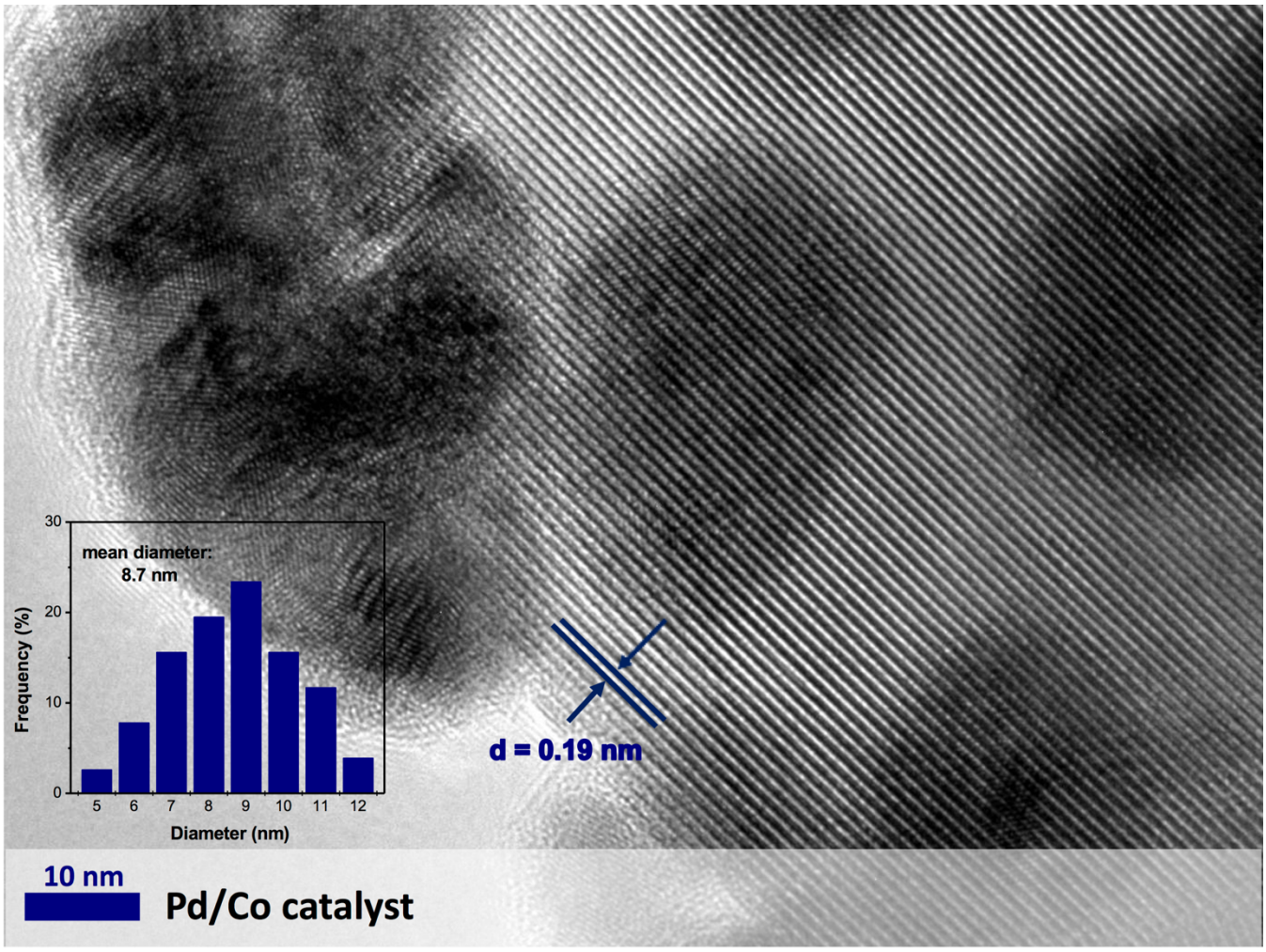

Figure 3 TEM image of the Pd/Co catalyst.

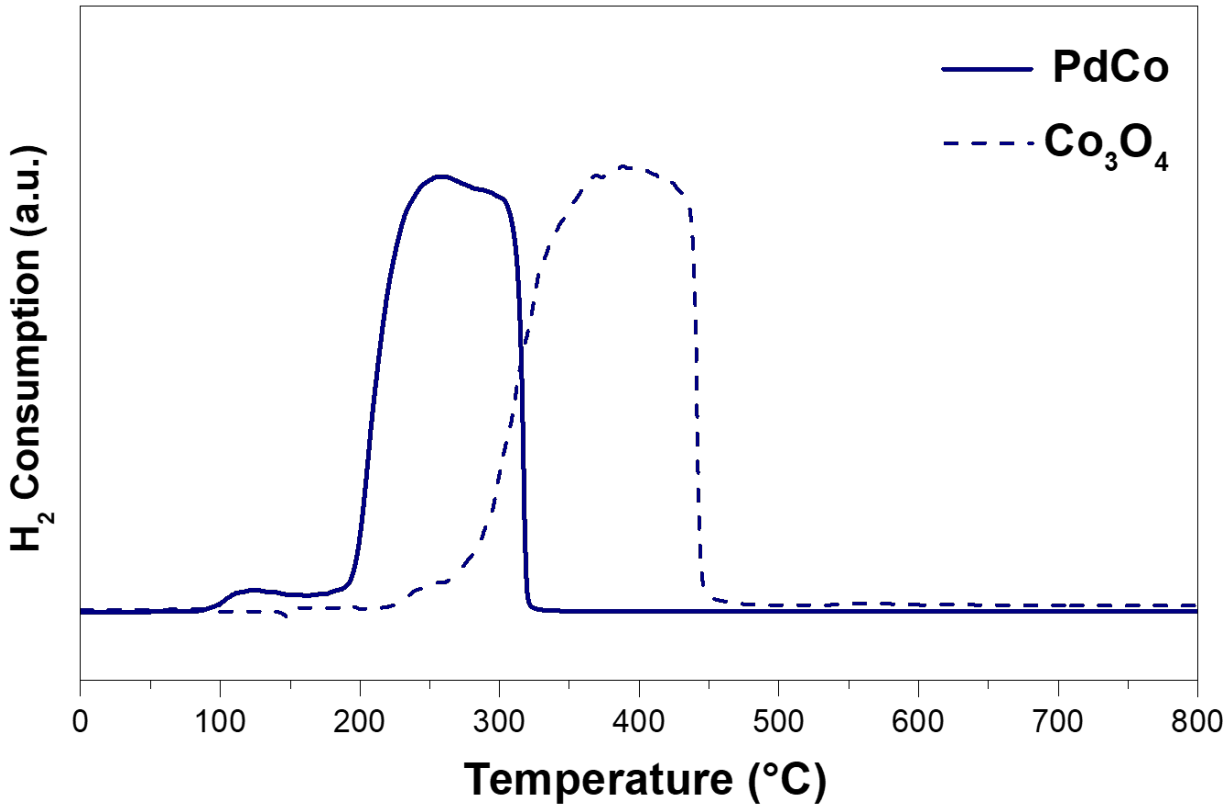

Figure 4 H_2-TPR profiles of unreduced Pd/Co and Co_3O_4 catalysts.

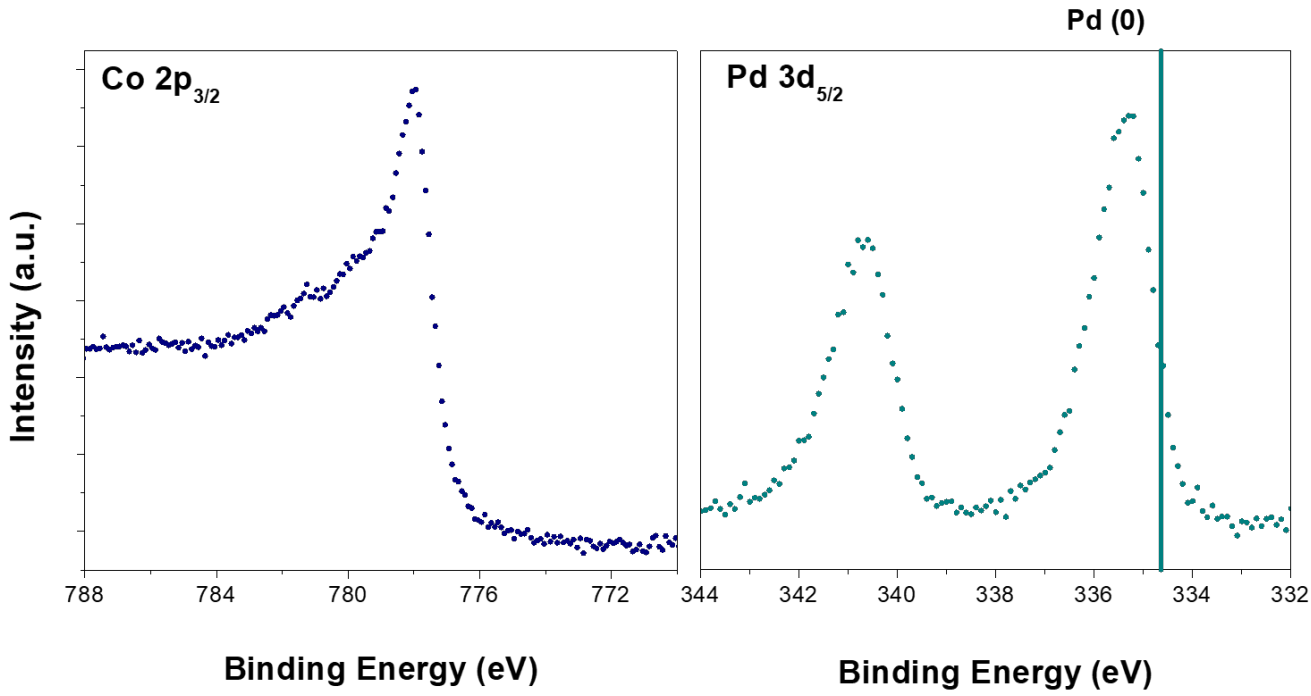

Figure 5 XPS plots of the reduced Pd/Co catalyst in Co $2p_{3/2}$ and Pd $3d_{5/2}$ levels.

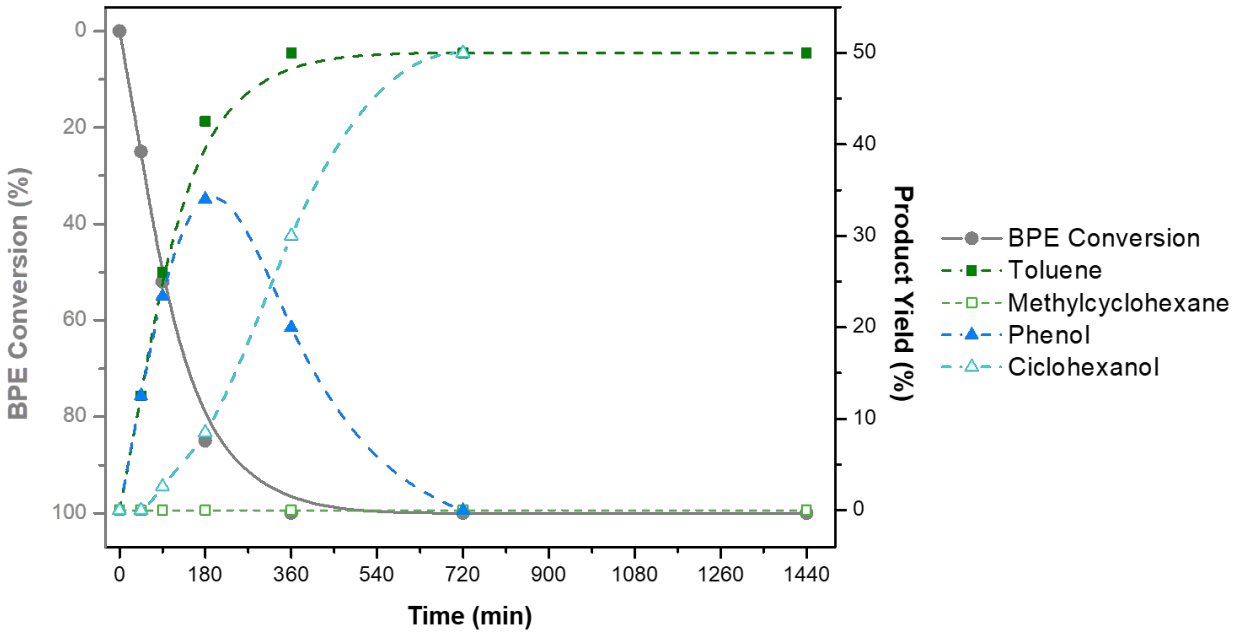

Figure 6. Product yields in the conversion of BPE with the Pd/Co catalyst under transfer hydrogenolysis conditions at 210°C against time (reaction conditions: 0.125 g of catalyst; 40 ml solution of BPE 0.1 M; N_2 pressure: 10 bar; stirring: 500 rpm).

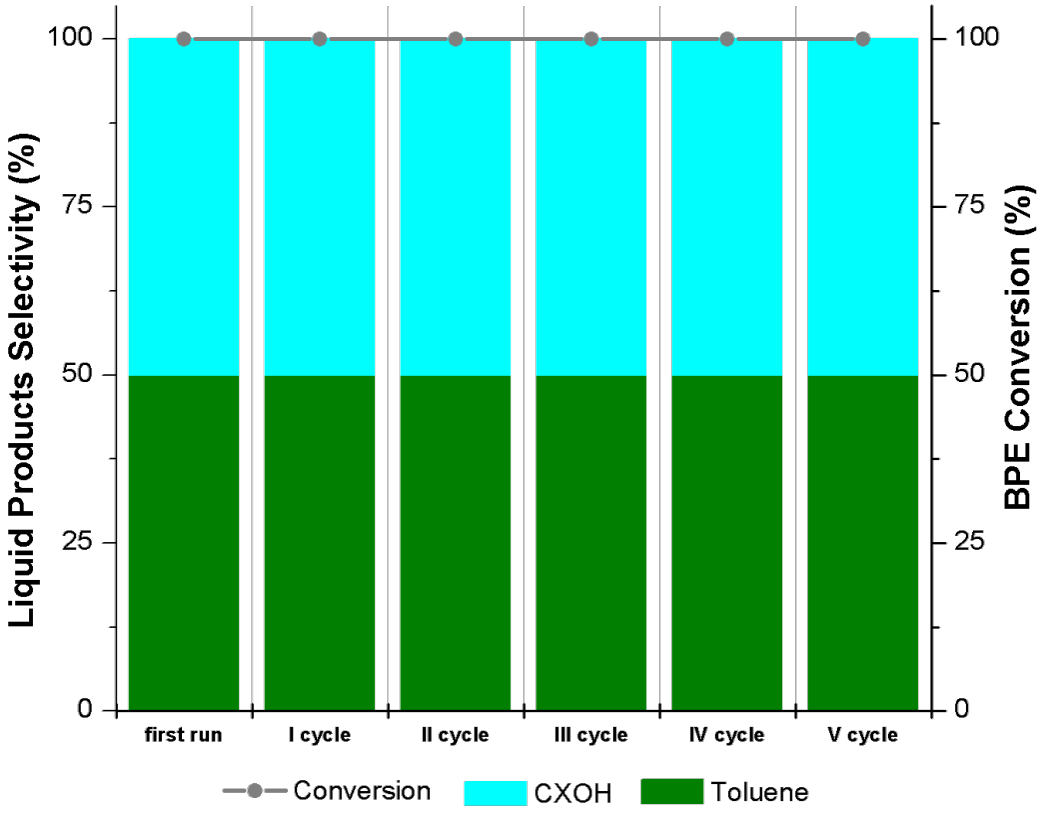

Figure 7. Recycling tests for Pd/Co catalyst in the CTH of BPE (reaction conditions: 0.125 g of catalyst; 40 ml solution of BPE 0.1 M; temperature: 240°C; time: 180 minutes; N_2 pressure: 10 bar; stirring: 500 rpm).

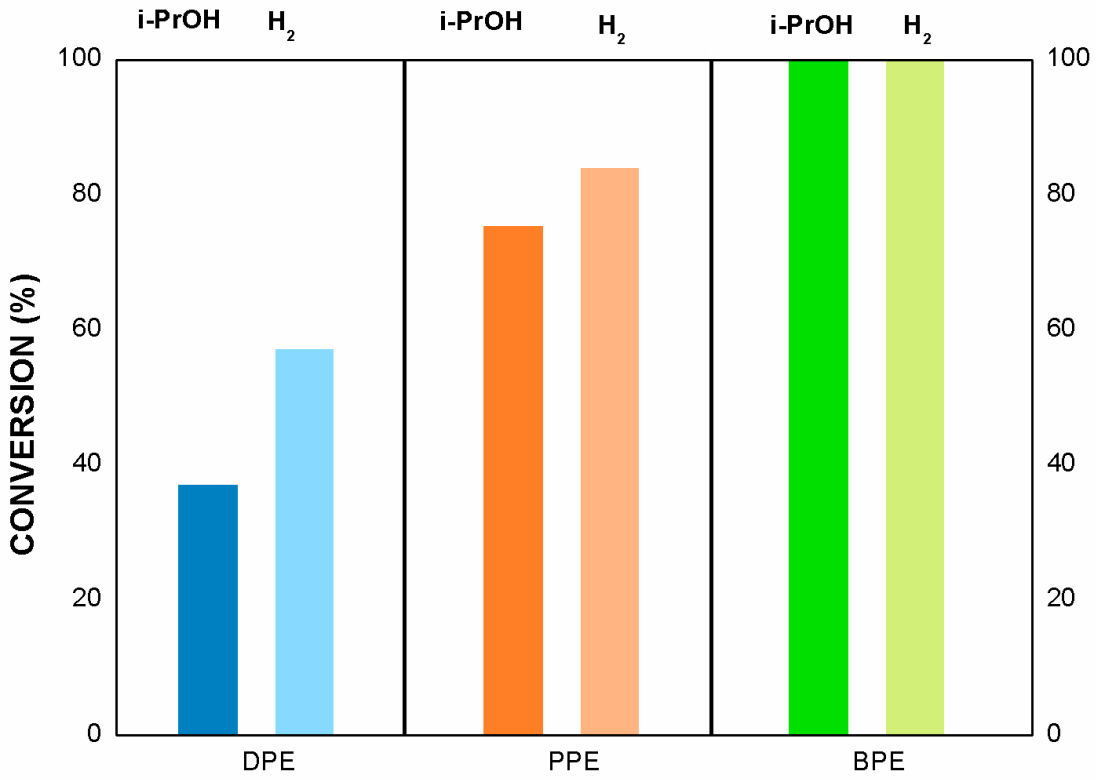

Figure 8. Conversion in the CTH and in the hydrogenolysis of BPE, PPE, and DPE (reaction conditions: 0.125 g of catalyst; 40 ml solution of BPE 0.1 M; temperature: 240°C; time: 180 minutes; N_2 or H_2 pressure: 10 bar; stirring: 500 rpm).

Table 1. Main characteristic of Pd/Co catalyst.

Catalyst notation	**S.A. [m^2/g]**	**Pd loading [%]**	**Pd-Co d_n [nm]**
Pd/Co	105	4.4	8.7

S.A: *surface area;* ***Pd loading [%]:*** *amount of palladium as determined by X-ray fluorescence (XRF) analysis;* ***Pd-Co d_n [nm]:*** *bimetallic palladium-cobalt mean particles size from TEM.*

Table 2. X-ray absorption fine structure characterization at the Pd K-edge for Pd/Co catalyst.

Catalyst	**Scattering Pair**	**CN**	**R (Å)**	**DW (Å)**	**R (%)**
Pd/Co	Pd-Pd	0,93	2,69	0,021	1,9
	Pd-Co	3,92	2,51	0,047	0,8

CN: *Coordination number;* ***R:*** *Interatomic distance;* ***DW:*** *Debye–Waller factor*

Table 3. Transfer hydrogenolysis of benzyl phenyl ether (BPE) in the presence of Pd/Co and Pd/C catalysts by using 2-propanol as H-source (reaction conditions: 0.125 g of catalyst; 40 ml solution of BPE 0.1 M; time: 180 minutes; N_2 pressure: 10 bar; stirring: 500 rpm)

Catalyst	Temperature [°C]	Conversion [%]	Chemoselectivity [%]				Aromatic Yield [%]
			TOL	MCX	PHE	CXO	
Pd/Co	240	100	50	-	-	50	50
Pd/C	240	45	50	-	40	10	41
Pd/Co	210	88	50	-	43	7	82
Pd/C	210	18	50	-	50	-	18
Pd/Co	180	30	50	-	50	-	30
Pd/C	180	-	-	-	-	-	-

***TOL**: Toluene; **MCX**: Methylcyclohexane; **PHE**:Phenol; **CXO**: Cyclohexanol*